

## Research Article

# Powder-Bed Stabilization for Powder-Based Additive Manufacturing

Andrea Zocca,<sup>1</sup> Cynthia M. Gomes,<sup>1</sup> Thomas Mühler,<sup>2</sup> and Jens Günster<sup>1,2</sup>

<sup>1</sup> Division of Ceramic Processing and Biomaterials, BAM Federal Institute for Materials Research and Testing, Unter den Eichen 44-46, 12203 Berlin, Germany

<sup>2</sup> Department for Engineering Ceramics, Clausthal University of Technology, Zehntnerstraße 2a, 38678 Clausthal-Zellerfeld, Germany

Correspondence should be addressed to Jens Günster; [jens.guenster@bam.de](mailto:jens.guenster@bam.de)

Received 27 February 2014; Accepted 28 April 2014; Published 16 June 2014

Academic Editor: Dachamir Hotza

Copyright © 2014 Andrea Zocca et al. This is an open access article distributed under the Creative Commons Attribution License, which permits unrestricted use, distribution, and reproduction in any medium, provided the original work is properly cited.

The most successful additive manufacturing (AM) technologies are based on the layer-by-layer deposition of a flowable powder. Although considered as the third industrial revolution, one factor still limiting these processes to become completely autonomous is the often necessary build-up of support structures. Besides the prevention of lateral shifts of the part during the deposition of layers, the support assures quality and stability to the built process. The loose powder itself surrounding the built object, or so-called powder-bed, does not provide this sustenance in most existent technology available. Here we present a simple but effective and economical method for stabilizing the powder-bed, preventing distortions in the geometry with no need for support structures. This effect, achieved by applying an air flow through the powder-bed, is enabling an entirely autonomous generation of parts and is a major contribution to all powder-based additive manufacturing technologies. Moreover, it makes powder-based AM independent of gravitational forces, which will facilitate crafting items in space from a variety of powdery materials.

## 1. Introduction

Additive manufacturing (AM) describes a class of technologies in which a 3D object is directly generated from a virtual model by adding material in a layer-by-layer approach defined by ASTM F2792-12a (Standard Terminology for Additive Manufacturing Technologies) as the “process of joining materials to make objects from 3D model data, usually layer upon layer, opposed to subtractive manufacturing methodologies, such as traditional machining” [1]. Well-known in the 80th and 90th as Rapid Prototyping, these technologies have been developed to reduce the time to market for new products by shortening the period between design and fabrication [2, 3]. While the need for flexibility in design had first priority at that time, nowadays the physical and functional properties of the generated parts are a major concern, for example, in emerging fields as tissue engineering [4], complex functional, and lightweight structures [5]. In this context even applications in space are currently being tested, where the diversity of tools and spare parts directly relates to the mass to be carried into space [6]. Accordingly,

the terminology for this class of technologies shifts gradually from Rapid Prototyping to Additive Manufacturing [7]. The philosophy behind AM is simple: a virtual data set and the choice of material are sufficient to build a part within a ubiquitous manufacturing process. In other words, the requirement of dedicated tooling and the need of adapting the manufacturing process to a certain geometry of the part to be built is obsolete. In the meanwhile, AM offers a broad repertoire of technologies for the manufacture of individual products and even the generation of structures unique to AM is possible. Moreover, additive manufacturing is a step further in the direction towards an autonomous manufacture, as the geometry of a part to be built does not imply a certain machine setup.

The material is typically fed into the process as a powder, paste, or liquid; that is, the material is in a state optimized for the layer deposition process, but not useful for defining a finite geometry. In the manufacturing process itself, the material is used to build up the desired object and it is simultaneously transferred into a state showing its final

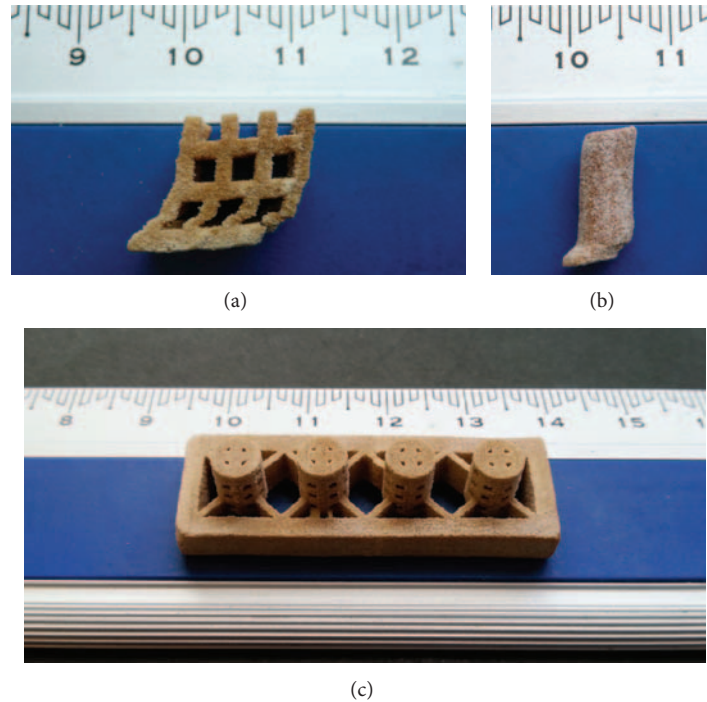


FIGURE 1: ((a), (b)) Ill-defined ceramic parts built without support structure distorted in the 3D printing process. (c) Parts designed with support structure.

physical properties or at least a mechanical strength sufficient to transfer the object built to further processing steps.

In powder-based AM technologies a solid structure is realized by the successive deposition of layers of a flowable powder. Briefly, a layer of powdered material is first spread and subsequently the corresponding layer information is selectively inscribed by, for example, local compaction or gluing; these steps are iteratively replicated until the object is completed. The layer information is defined by the corresponding cross section of a sliced virtual 3D model of the object to be built. At the end, the part is completely embedded in a powder-bed, from which it can be easily extracted and cleaned.

The technology used to inscribe the layer information depends on the specific process considered: two of the most well-known and world-spread processes are the “three-dimensional printing (3DP)” and the “selective laser sintering (SLS)” [8].

The milestone patent “three-dimensional printing techniques” [9] by Sachs et al. was filed in 1989, while Deckard’s patent “method and apparatus for producing parts by selective sintering” [10] dates back three years earlier. The former method uses a printing head to selectively spread out droplets of a liquid binder, while the latter employs the energy of a focused laser beam to selectively sinter/melt a powder.

Since the first pioneering applications, many developments have been introduced, greatly extending the use of different materials [11–13], improving the physical properties of the components built, and enhancing the accuracy of the process [14], thus allowing novel applications [15]. Still very important issues remain nowadays, hampering a completely

autonomous production of parts and even restricting the freedom of design by means of these technologies. One of the major issues is the stability of the parts during the building process, which implies the need of support structures in most of the AM technologies. Support structures are structures which are built up mainly for the fixation of the desired geometry within the powder-bed. Actually, one of the intrinsic features of the powder-based technologies is the ability of the powder-bed to support the generated parts against gravitation. Despite of this, it is not stable enough to act against forces originating from powder deposition, resulting in a lateral displacement of the object upon subsequent deposition of layers; see Figures 1(a) and 1(b). These forces, which according to most setups are perpendicular to the gravitational force and tangential to the powder-bed’s surface, cause the part to shift along the direction of the movement of the deposition unit, which is normally a blade or a roller unit. Therefore, to prevent this effect, support structures are commonly built along with the part, Figure 1(c).

Building up support structures consumes processing time and wastes material. Their removal requires an additional postprocessing, which is again time consuming and involves a dedicated treatment of each individual component. In the case of “selective laser sintering/melting (SLS/SLM)” the tight fixation by such structures causes also internal stresses that can potentially deform the component after its release. Very recently some work has approached this problem from a designer’s perspective suggesting an optimization of the parts geometry [16] or of the materials used [17], with the aim of avoiding the use of support structures; other works focused instead on the optimization of the support structures itself

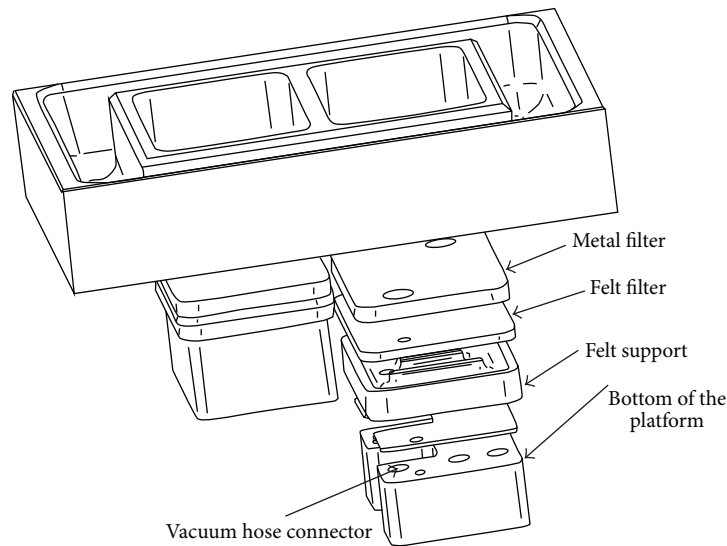


FIGURE 2: Exploded assembly drawing of the vacuum 3D print setup.

[18, 19]. Both approaches impose restrictions to the freedom in design and clearly have their limitations, as they do not tackle the root cause of the problem.

Obviously there exists a clear need for process improvements that are able to overcome the instability of the powder-bed and, thus, enable an entirely autonomous fabrication process. The application of a gas flow through the powdery material can indeed stabilize the powder-bed to an extent making support structures dispensable. Moreover, it makes the process independent of gravitational forces, facilitating the advantageous application of powder-based AM in space. This work introduces this innovative approach as well as the first results related to the production of parts without need of support structures.

## 2. Materials and Methods

A commercial 3D printer (RX-1, ExOne, USA) has been modified in order to implement a vacuum setup. This setup is described in detail in the Results and Discussion section (see also Figure 2).

The vacuum pump used is a rotary two-stage pump (PZ, Welch-Ilmvac GmbH, Ilmenau, Germany) with a pumping capacity of  $10 \text{ m}^3/\text{h}$ , while the metal filter was machined from a sheet 5 mm in thickness, purchased from GKN Sinter Metals Filters GmbH, 42477 Radevormwald, Germany. All the other components were designed and CNC machined in house.

Two ceramic powders have been compared in a set of experiments, in order to study the effect of the vacuum setup on the layer-by-layer deposition of the powder-bed in the 3D printer.

A lithium aluminosilicate (LAS) glass frit was provided by Colorobbia S.p.a (Sovigliana Vinci, Firenze, Italy) [20]. More information about the 3D printing of this material can be found in the references [21]. The frit was attrition milled and sieved between  $63 \mu\text{m}$  and  $125 \mu\text{m}$ .

An  $\text{Al}_2\text{O}_3$  powder (Gilox 63, Almatix GmbH, Ludwigshafen, Germany) presents, according to the producer's specifications, a  $d_{10} = 2,5 \mu\text{m}$ ;  $d_{50} = 17 \mu\text{m}$ ;  $d_{90} = 45 \mu\text{m}$ .

The density of the powder-bed was determined by weighing the powder after a deposition of 50 layers (each  $100 \mu\text{m}$  thick) in the printer's building platform and dividing the mass by the geometrical volume obtained.

The density measurements were run on triplicates and the values compared by one-tailed Student's  $t$ -test. A value of  $P < 0.01$  was considered significant, but the exact  $P$  values are also reported. All results are reported as mean  $\pm$  standard deviation.

A proprietary bioceramic was also used to demonstrate the three-dimensional printing of complex-shaped parts using this setup, without the use of support structures. This composition is a fast resorbable calcium alkali orthophosphate ceramic; detailed information about this material can be found elsewhere [22, 23]. The powder used in the experiments was granulated starting from particles ( $d_{50} = 7 \mu\text{m}$ ) and 5 wt% PVA as binder in a fluidized bed granulator. The granules were sieved between  $45$  and  $90 \mu\text{m}$  before printing.

## 3. Results and Discussion

In order to apply an air flow through the powder-bed in a 3D printing process, a commercial 3D printer has been modified according to the proprietary setup in Figure 2: the bottom side of the building platform is connected to a vacuum pump applying vacuum to one side of the powder-bed, resulting in a pressure gradient which creates then an air flow through the powder. A filter made of porous sinter-steel (average pore diameter =  $10 \mu\text{m}$ ) acts as building base and prevents the powder from being sucked into the pumping unit. The effect of the applied vacuum can be appreciated in the video provided with the Supplementary Material available online at <http://dx.doi.org/10.1155/2014/491581>.

TABLE 1: Bulk density and powder-bed density of powders A and B, with and without the application of the vacuum setup. Comparison of powders A and B freely settled bulk densities according to Hausner method and densities of powder beds composed out of 50 layers, each 100  $\mu\text{m}$  in thickness.

|   | Powder A: density ( $\text{g}/\text{cm}^3$ )<br>(relative density, %) | Powder B: density ( $\text{g}/\text{cm}^3$ )<br>(relative density, %) |
|---|---|---|
| Bulk density  |   |   |
| Free settled  | 1,02 $\pm$ 0,01 (43,4 %)  | 1,23 $\pm$ 0,02 (31,1 %)  |
| Tapped  | 1,23 $\pm$ 0,01 (52,3 %)  | 1,73 $\pm$ 0,01 (43,8 %)  |
| Hausner ratio   | 1,20 $\pm$ 0,02   | 1,41 $\pm$ 0,03   |
| Powder-bed density<br>(50 layers deposited by roller) |   |   |
| With vacuum   | 1,16 $\pm$ 0,01 (49,4 %)  | 1,70 $\pm$ 0,07 (43,0 %)  |
| Without vacuum  | 1,09 $\pm$ 0,02 (46,4 %)  | 1,15 $\pm$ 0,02 (29,1 %)  |

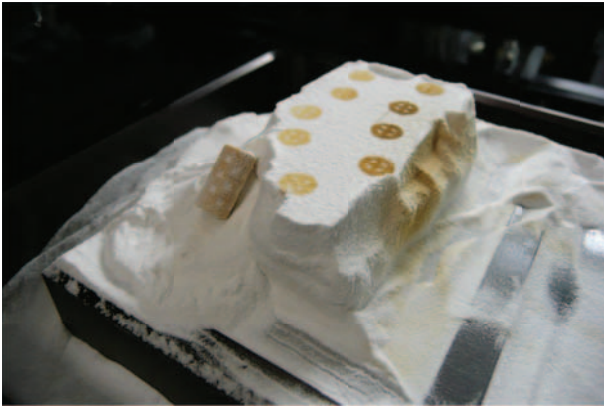


FIGURE 3: Set of cylinders, revealing a designed ordered porosity, printed applying the described setup, without the use of support structures. Powder used: granulated powder sieved between 45 and 90  $\mu\text{m}$  of a proprietary bioceramic.

The air flow through the powder provides an additional force in direction to the porous building base and first experiments have proven that it is sufficient to stabilize the powder-bed, making support structures dispensable; see also Figure 3.

Figure 3 shows a set of cylinders (diameter = 5 mm, height = 12 mm) revealing a designed ordered porosity that were printed applying the described setup and without the use of support structures. The cylinders show no deformation or distortion. The material used was a granulated powder (sieved between 45 and 90  $\mu\text{m}$ ) of a proprietary bioceramic system.

Besides the powder-bed stabilization, the modified setup improves also the powder flow and its compaction during the layer formation process.

From a fundamental physics point of view, the flowing behavior of a powder depends on the interplay between the attractive interparticle force,  $F_a$ , and the gravitational force acting on each individual particle, which is directly related to the particle weight,  $m_g$ . The ratio between these two forces defines the cohesive granular Bond number,  $\text{BN} = F_a/m_g$  [24].

Flowability greatly depends on the bond number BN, because if particulates receive a gravitational force much larger than the attractive interparticle force (small BN), they follow gravitation irrespective of an existing interparticle attraction. As a consequence flowable powders pack well [25].

In order to quantify the effect of an air stream through the powder-bed, the layer-by-layer deposition of two different powders was studied: a glass powder (type A), with a rather coarse particle size distribution (63–125  $\mu\text{m}$ ) and good flowability and a fine  $\alpha\text{-Al}_2\text{O}_3$  powder (type B), with an average size of 17  $\mu\text{m}$  and typically poor flowability.

The flowability of the two powders was quantified according to the Hausner Ratio [26]:

$$\text{HR} = \frac{\rho_{\text{Tap}}}{\rho_{\text{Bulk}}} \quad (1)$$

with  $\rho_{\text{Bulk}}$  being the freely settled bulk density of the powder and  $\rho_{\text{Tap}}$  being the plateau tap density reached after a certain number of tapping cycles, in  $\text{g}/\text{cm}^3$ . This method was chosen, besides its simplicity, as it directly relates the powder packing density to its flowability. In fact, well flowable powders already reach a high bulk density when they are freely settled, and the increase of density after tapping is lower than for nonflowable powders. Hence, well flowable powders have a lower Hausner ratio than nonflowable powders.

The measured bulk densities and Hausner ratios for powders of type A and type B, reported in Table 1, clearly reveal that the type A powder flows and packs significantly better than type B (higher HR). The determined HR is in accordance with the previous values associated with good and poor flowabilities [26].

In order to evaluate the processability of the two powders, the density of a powder-bed composed of 50 layers each 100  $\mu\text{m}$  thick was measured. For buildup of the layered structure, a commercial 3D printer was employed. The printer uses a counter rotating roller for depositing the individual layers. The obtained densities with and without the application of vacuum are presented in Table 1.

It is noteworthy that, according to Table 1, even without the application of vacuum the rolling deposition has a subtle but significant effect on the powder compaction. The powder-bed for powder A has a higher density compared to the free

settled powder ( $+6 \pm 2\%$ ), while the powder-bed for powder B has a lower density than the free settled powder ( $-6 \pm 2\%$ ).

This trend is related to the different flowing behavior of the powders, where the flowable powder A can be effectively deposited and compacted by means of the roller, whilst the deposition of the poorly flowable powder B results in a poorly packed powder-bed.

The effect of the application of vacuum on the density of the powder-bed was also evaluated for the two powders. In both cases, there was a significant increase in density when applying vacuum, that is,  $+48 \pm 2\%$  for powder B and  $+6 \pm 2\%$  for powder A. The hypothesis that the density of the powder-bed with the application of vacuum is higher than the density of the powder-bed without the application of vacuum was supported statistically by a one-tailed Student's *t*-test, yielding a significance level of *P* value =  $1.9 \times 10^{-3}$  for powder A and *P* value =  $8.5 \times 10^{-5}$  for powder B.

The increase in density, when vacuum was applied, was much higher for powder B than for powder A. This observation highlights the positive effect of the applied vacuum on the powder compaction especially on fine powders, which typically show a poor flowability.

It is noticeable that the density of the powder-bed for powder B, when vacuum was applied, reaches a value of  $1.70 \text{ g/cm}^3$  that corresponds to about 43% of the theoretical density of  $\alpha\text{-Al}_2\text{O}_3$ . Such value is particularly remarkable since it is similar to the tapped density of this same powder, which was  $1.73 \text{ g/cm}^3$ . Furthermore, when vacuum was applied, the relative densities of the powder-beds for powders A (49.4%) and B (43.0%) are comparable. Instead, when vacuum was not applied, the relative densities are considerably different (29.1% and 46.4% theoretical density for powders B and A, resp.).

The effective packing under the influence of a gas flow through the powder-bed can be understood within the framework of a model taking into account the forces active on each individual particle during the layer deposition process. As the vacuum is applied from the bottom side of the powder-bed, see also Figure 2, the sum of all forces averaged over the particles yields a total average force in direction to the building platform and, thus, parallel to gravitation. This observation is intuitively consistent with a macroscopic picture, with the powder simply sucked towards the porous building platform. Within this picture, however, one cannot expect a significant compaction of the powder, as the acting forces are small compared to forces applied in established technologies for compaction of powders. On the other hand, local forces induced by applying an air flow through the powder-bed guide the particles to effectively fill the interstices, as they are acting on the particles already when they are not yet in direct contact with the neighboring particles, that is, in the flowing state during the layer deposition. This effect is existing irrespective of the action of gravitational forces, which, in turn, facilitates powder-based AM under zero gravity.

The effect of external forces on the packing behavior of calcined alumina with different particle size distributions is already known in the literature. Mechanically dried

filter-cake of deflocculated fine-grained alumina presents higher packing fractions if the powder has larger geometric standard deviation. The packing density depends significantly on the form of the size distribution and also on the range of the particle size [27]. Different models (e.g., [28] or [29]) can be used to predict these effects on the degree of densification of a powder compact without and with application of external forces, for example, tapping cycles. Ideally, if the particle size decreases, the proportion of fines must increase in order to fill the interstices between coarser particles, increasing though the packing fraction [27]. This effect is accentuated during the stabilization with vacuum, since it helps the finer particles to migrate between the interstices of the coarser ones. It has been observed that powders with a wide size distribution in the range of  $20\text{--}50 \mu\text{m}$ , and large amounts of fines, have limited the effect of the air flow to only few millimeters height, because the powder-bed becomes quickly clogged by the finer particles filling the voids between the coarser.

However, it should be noted that the stabilization effect of vacuum is active for powder-beds up to 100 mm, in the case of powders with a coarse grain size ( $>50 \mu\text{m}$ , such as powder type A) and small amounts of fines. Powders with smaller grain sizes should present low proportion of fines or a tighter particle size distribution.

Further studies and simulations will be devoted to the understanding of the interplay between air flow and the formation of the powder-bed, such as the formation of preferential paths within the powder.

## 4. Conclusions

The application of an air flow through the powder has been demonstrated as an effective method for stabilizing the powder-bed during the layer-by-layer deposition. A proprietary setup has been applied to a commercial 3D printer, allowing the manufacturing of three-dimensional ceramic parts without the use of support structures. Moreover, it was found that the application of this setup can increase the density of the powder-bed, especially in the case of the deposition of nonflowable powders.

This setup could be easily adapted to other additive manufacturing technologies (e.g., SLS) and to other materials (e.g., metals), allowing an improved control over the geometry of the parts without the need of support structures, thus enabling a completely autonomous powder-based additive manufacturing process.

## Conflict of Interests

The authors declare that there is no conflict of interests regarding the publication of this paper.

## References

- [1] ASTM Standard F2792, *Standard Terminology for Additive Manufacturing Technologies*, ASTM International, West Conshohocken, Pa, USA, 2012.

- [2] E. Sachs, M. Cima, P. Williams, D. Brancazio, and J. Cornie, "Three dimensional printing. Rapid Tooling and prototypes directly from a CAD model," *Journal of Engineering for Industry*, vol. 114, no. 4, pp. 481–488, 1992.
- [3] D. T. Pham and R. S. Gault, "A comparison of rapid prototyping technologies," *International Journal of Machine Tools and Manufacture*, vol. 38, no. 10-11, pp. 1257–1287, 1998.
- [4] S. J. Hollister, "Porous scaffold design for tissue engineering," *Nature Materials*, vol. 4, no. 7, pp. 518–524, 2005.
- [5] D. W. Rosen, "Computer-aided design for additive manufacturing of cellular structures," *Computer-Aided Design & Applications*, vol. 4, no. 1–6, pp. 585–594, 2007.
- [6] M. Snyder, J. Dunn, and E. Gonzalez, "The effects of microgravity on extrusion based additive manufacturing," in *Proceedings of the AIAA SPACE Conference and Exposition*, September 2013.
- [7] D. Bak, "Rapid prototyping or rapid production? 3D printing processes move industry towards the latter," *Assembly Automation*, vol. 23, no. 4, pp. 340–345, 2003.
- [8] D. L. Bourell, H. L. Marcus, J. W. Barlow, and J. J. Beaman, "Selective laser sintering of metals and ceramics," *International Journal of Powder Metallurgy*, vol. 28, no. 4, pp. 369–381, 1992.
- [9] E. M. Sachs, J. S. Haggerty, M. J. Cima, and P. A. Williams, "Inventors, Massachussets Institute of Technology, Assignee. Three-dimensional printing techniques," US Patent no. 5,204,055, April 1993.
- [10] C. R. Deckard, "Inventor, Board of Regents, The University of Texas System, Assignee. Method and apparatus for producing parts by selective sintering," US Patent no. 4,863,538, September 1989.
- [11] S. Kumar and J.-P. Kruth, "Composites by rapid prototyping technology," *Materials and Design*, vol. 31, no. 2, pp. 850–856, 2010.
- [12] P. Calvert, "Materials science: printing cells," *Science*, vol. 318, no. 5848, pp. 208–209, 2007.
- [13] T. F. Wegrzyn, M. Golding, and R. H. Archer, "Food Layered Manufacture: a new process for constructing solid foods," *Trends in Food Science & Technology*, vol. 27, no. 2, pp. 66–72, 2012.
- [14] I. Yadroitsev, I. Shishkovsky, P. Bertrand, and I. Smurov, "Manufacturing of fine-structured 3D porous filter elements by selective laser melting," *Applied Surface Science*, vol. 255, no. 10, pp. 5523–5527, 2009.
- [15] N. Jones, "Science in three dimensions: the print revolution," *Nature*, vol. 486, no. 7405, pp. 22–23, 2012.
- [16] C. Yan, L. Hao, A. Hussein, and D. Raymont, "Evaluations of cellular lattice structures manufactured using selective laser melting," *International Journal of Machine Tools and Manufacture*, vol. 62, pp. 32–38, 2012.
- [17] K. Mumtaz, P. Vora, and N. Hopkinson, "A method to eliminate anchors/supports from directly laser melted metal powder bed processes," in *Proceedings of the 22nd International Solid Freeform Fabrication Symposium*, Austin, Tex, USA, 2011.
- [18] A. Hussein, L. Hao, C. Yan, R. Everson, and P. Young, "Advanced lattice support structures for metal additive manufacturing," *Journal of Materials Processing Technology*, vol. 213, no. 7, pp. 1019–1026, 2013.
- [19] J. Jhabvala, E. Boillat, C. André, and R. Glardon, "An innovative method to build support structures with a pulsed laser in the selective laser melting process," *International Journal of Advanced Manufacturing Technology*, vol. 59, no. 1–4, pp. 137–142, 2012.
- [20] G. Baldi, G. Borelli, A. Antonini, and M. Bitossi, "Inventors, Colorobbia Italia S.P.a., Assignee. Process for the preparation of ceramic glass material in the form of sheets, sheets thus obtained and use thereof," Patent application US, 2010/0069218 A1, March 2010.
- [21] A. Zocca, C. M. Gomes, E. Bernardo, R. Müller, J. Günster, and P. Colombo, "LAS glass-ceramic scaffolds by three-dimensional printing," *Journal of the European Ceramic Society*, vol. 33, no. 9, pp. 1525–1533, 2013.
- [22] G. Berger, R. Gildenhaar, and U. Ploska, "Rapid resorbable, glassy crystalline materials on the basis of calcium alkali orthophosphates," *Biomaterials*, vol. 16, no. 16, pp. 1241–1248, 1995.
- [23] R. Gildenhaar, C. Knabe, C. Gomes, U. Linow, A. Houshmand, and G. Berger, "Calcium alkaline phosphate scaffolds for bone regeneration 3Dfabricated by additive manufacturing," *Key Engineering Materials*, vol. 493-494, pp. 849–854, 2012.
- [24] S. T. Nase, W. L. Vargas, A. A. Abatan, and J. J. McCarthy, "Discrete characterization tools for cohesive granular material," *Powder Technology*, vol. 116, no. 2-3, pp. 214–223, 2001.
- [25] A. Castellanos, "The relationship between attractive interparticle forces and bulk behaviour in dry and uncharged fine powders," *Advances in Physics*, vol. 54, no. 4, pp. 263–276, 2005.
- [26] H. H. Hausner, "Powder characteristics and their effect on powder processing," *Powder Technology*, vol. 30, no. 1, pp. 3–8, 1981.
- [27] J. S. Reed, *Principles of Ceramics Processing*, Wiley, New York, NY, USA, 1995.
- [28] A. H. M. Andreasen, "Ueber die Beziehung zwischen Kornabstufung und Zwischenraum in Produkten aus losen Körnern (mit einigen Experimenten)," *Kolloid-Zeitschrift*, vol. 50, no. 3, pp. 217–228, 1930.
- [29] J. E. Funk and D. R. Dinger, *Predictive Process Control of Crowded Particulate Suspensions Applied to Ceramic Manufacturing*, Kluwer Academic Publishers, Norwell, Mass, USA, 1994.